# Two Target Detection Algorithms for Passive Multistatic Radar

Jun Liu, *Member, IEEE*, Hongbin Li, *Senior Member, IEEE*, and Braham Himed, *Fellow, IEEE*

***Abstract*—This paper considers the problem of passive detection with a multistatic radar system involving a noncooperative illuminator of opportunity (IO) and multiple receive platforms. An unknown source signal is transmitted by the IO, which illuminates a target of interest. These receive platforms are geographically dispersed, and collect independent target echoes due to the illumination by the same IO. We consider a generalized canonical correlation (GCC) detector for passive detection which requires the knowledge of the noise power. We derive closed-form expressions for the probabilities of false alarm and detection of this detector. For the case where the noise power is unknown, we propose a generalized likelihood ratio test (GLRT) detector to deal with the passive detection problem. Moreover, a closed-form expression for the probability of false alarm of this GLRT detector is given, which shows that the proposed GLRT detector exhibits a constant false alarm rate property with respect to the noise power. Numerical simulations demonstrate that the proposed GLRT detector generally outperforms the generalized coherence detector, a previous popular passive detector that neither requires the knowledge of the noise power. In addition, the GLRT also outperforms the GCC detector when the latter has an uncertainty in its knowledge of the noise power.**

***Index Terms*—Complex Wishart matrix, generalized coherence, generalized likelihood ratio test, opportunistic illuminator, passive detection, passive multistatic radar.**

## I. Introduction

A passive radar system can detect and track a target of interest by exploiting readily available, non-cooperative illuminators of opportunity (IOs) [1]–[4], which is of great interest in both civilian and military scenarios due to a number of advantages. First, this system is substantially smaller and less expensive compared to an active radar system because it does not need a transmitter. Second, the bistatic or multistatic configuration enables it to obtain spatial diversity of the targets' radar cross section (RCS), which leads to potential gains in detection and classification capabilities [5]. Finally, many IOs are available for passive sensing, such as frequency modulation radio [6]–[8], television [9], [10], cell phone base stations [11], digital audio broadcasting (DAB) [12], digital video broadcasting-terrestrial (DVB-T) [13]–[15], and second generation digital video broadcasting-terrestrial (DVB-T2) sources [16].

Due to the non-cooperative nature of the IO, the transmitted signal is out of control and generally unknown to a passive receiver. As a result, a conventional matched filter cannot be implemented for detection. In many passive radar systems, an additional separate channel, referred to as the reference channel (RC), is usually equipped to collect the transmitted signal as a reference for passive detection. This reference signal can be used to eliminate unwanted echoes in surveillance channels (SCs), e.g., direct signals, clutter, and multi-path signals [17]–[21]. For target detection, the reference signal can also be heuristically employed to conduct delay-Doppler cross-correlation operation with the surveillance signal [3], [17], [22]. Nevertheless, the performance is significantly degraded when the reference signal is noisy. To deal with the lack of knowledge of the signal transmitted from the IO, a different approach is to employ multiple SCs in a passive radar system [23]. Since these SCs collect target echoes due to the illumination of the same IO, a correlation exists among the observations collected by the SCs, which can be employed for passive detection. In the following, we focus on target detection in a passive radar system with multiple SCs.

A passive radar system may have a monostatic or multistatic configuration. A monostatic passive radar system usually consists of a single receive platform, while a multistatic one is comprised of multiple spatially separated receivers. In general, a multistatic passive radar system has a better performance than a monostatic counterpart due to the following reasons. First, in the multistatic passive radar system, the receivers are geographically distributed such that independent observations of a target from multiple different aspects are possible, which brings about the so-called spatial diversity. This spatial diversity can be used to reduce significantly the scintillations of the target's RCS. Second, multiple receivers are able to collect more data samples over a given observation time. It is of significant importance for a passive system exploiting low-power IOs, since many IOs may have a low power in practice. For example, a broadcast station usually uses an approximately isotropic antenna to transmit a signal to cover a broad area, which leads to no directional gain in its transmit antenna and low-power illumination to the target [24].

Manuscript received January 01, 2014; revised May 12, 2014; accepted September 10, 2014. Date of publication September 19, 2014; date of current version October 23, 2014. The associate editor coordinating the review of this manuscript and approving it for publication was Prof. Hongwei Liu. This work was supported in part by a subcontract with Dynetics, Inc. for research sponsored by the Air Force Research Laboratory (AFRL) under Contract FA8650-08-D-1303.

J. Liu was with the Department of Electrical and Computer Engineering, Stevens Institute of Technology. He is now with the National Laboratory of Radar Signal Processing, Xidian University, Xi'an, 710071, China (e-mail: jun_liu_math@hotmail.com; junliu@xidian.edu.cn).

H. Li is with the Department of Electrical and Computer Engineering, Stevens Institute of Technology, Hoboken, NJ 07030 USA (e-mail: hongbin.li@stevens.edu).

B. Himed is with AFRL/RYMD, Dayton, OH 45433 USA (e-mail: braham.himed@wpafb.af.mil).

Color versions of one or more of the figures in this paper are available online at http://ieeexplore.ieee.org.

Digital Object Identifier 10.1109/TSP.2014.2359637

The target detection problem in a passive multistatic radar system is equivalent to determining the presence or absence of a common but unknown signal with independent noisy observations from multiple receivers. Studies of this and similar detection problem can be traced to [25]–[28], where a magnitude-squared coherence (MSC) detector is developed for a two-channel signal detection. The MSC is a normalized cross-spectral density function and measures the coherence between two stationary stochastic processes. Further studies on the properties of the MSC can be found in [29]–[31]. To handle the detection problem in the case of multiple channels, a generalized coherence (GC) is proposed in [32], [33] as an extension of the MSC. Its probability of false alarm has a simple form [34], and is independent of the noise power. Hence, the GC detector bears a constant false alarm rate (CFAR) property against the noise power. The asymptotic performance analysis of the GC detector is provided in [35]. Recently, the GC detector is also derived from a Bayesian perspective [36].

For a passive multistatic radar system with a single IO, the authors in [1] propose the generalized canonical correlation (GCC) detector for passive detection with known noise power. This detector is exactly the largest eigenvalue of the Gram matrix or covariance matrix of the signals received by the multistatic radar system. The GCC detector can also be applied in a single frequency network with multiple transmitters emitting a common unknown signal [37]. It is worth noticing that the same detector as the GCC in [1] is independently derived in [2] for the detection of low probability of intercept signals using distributed sensors. However, the performance analysis of the GCC is not provided in [1], [2], or [37].

The purpose of this paper is two-fold. One is to develop a GLRT detector for the case of unknown noise power in passive multistatic radars, since in practice knowledge of the noise power is often unavailable *a priori*. It is shown that the proposed GLRT detector is associated with all eigenvalues of the Gram matrix of the received signals. A closed-form expression for the probability of false alarm of the proposed GLRT detector is obtained, which indicates that the proposed GLRT detector exhibits a CFAR property with respect to the noise power. The second objective is to provide a performance analysis of the detector of [1], [2], [37], which is considered as a benchmark for our proposed GLRT detector, since the former assumes knowledge of the noise power. We derive closed-form expressions of the probabilities of false alarm and detection for this detector. Simulation results demonstrate that the proposed GLRT detector outperforms the GC detector in cases where the number of receive platforms is large (greater than 3). In addition, the proposed GLRT detector with unknown noise power provides improved detection performance, compared with the GCC detector proposed with known noise power in [1], in the case where there exists an uncertainty in the noise power.

The remainder of this paper is organized as follows. Section II establishes the signal model. We investigate the detection problem for the cases of unknown and known noise powers in Sections III and IV, respectively. Simulation results are illustrated in Section V and finally the paper is summarized in Section VI.

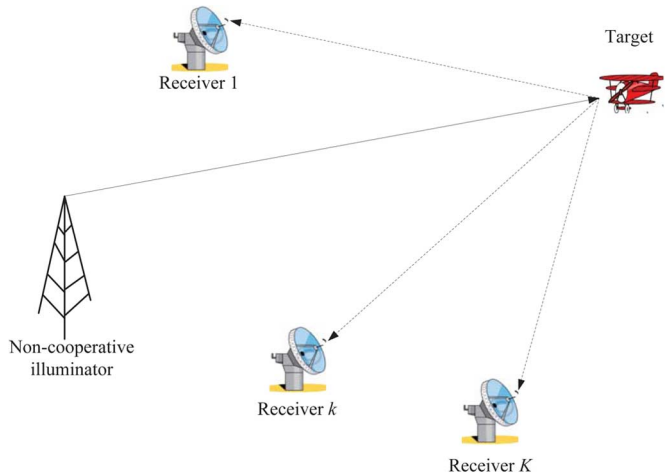


Fig. 1. Configuration of a multistatic passive radar system.

*Notation:* Vectors (matrices) are denoted by boldface lower (upper) case letters. Superscripts $(\cdot)^T$ and $(\cdot)^\dagger$ denote transpose and complex conjugate transpose, respectively. The notation $\sim$ means "is distributed as," and $\mathcal{CN}$ denotes a circularly symmetric, complex Gaussian distribution. $\mathbf{I}_p$ stands for a $p$-dimensional identity matrix. $|\cdot|$ represents the modulus of a complex number, $\|\cdot\|$ is the Frobenius norm, and $\jmath = \sqrt{-1}$. $\det\{\cdot\}$ and $\mathrm{tr}\{\cdot\}$ denote the determinant and trace of a matrix, respectively. $\mathrm{C}_n^m$ and $(n)_k$ are the binomial coefficient and the Pochhammer symbol, respectively. $u(\cdot)$ and $\Gamma(\cdot)$ denote the Heaviside step function and Gamma function, respectively. $\lambda_K(\mathbf{A}) \leq \lambda_{K-1}(\mathbf{A}) \leq \cdots \leq \lambda_2(\mathbf{A}) \leq \lambda_1(\mathbf{A})$ denote the ordered eigenvalues of $K$-dimensional matrix $\mathbf{A}$. The $(i,j)$th entry of matrix $\mathbf{A}$ is represented by $\mathbf{A}_{i,j}$.

## II. Signal Model

Consider a passive multistatic radar system as shown in Fig. 1, which involves one non-cooperative transmitter (i.e., IO) and $K$ geographically dispersed receivers or sensors are deployed to collect the echoes of a target of interest due to the illumination of the IO.

Denote by $s(n)$ for $n = 1, 2, \ldots, N$ the unknown signal transmitted by the non-cooperative IO in the discrete time domain. Assume that in each receiver the direct signal from the IO has been removed by using a directional antenna or some signal processing techniques [17], [21]. The signal received in the $k$th receiver, denoted by $x_k(n)$, can be expressed as [23]

$$x_k(n) = \alpha_k s(n - n_k) \exp(\jmath\, \Omega_k n) + w_k(n), \qquad (1)$$

where $n = 1, 2, \ldots, N$, $k = 1, 2, \ldots, K$, $\alpha_k$ is a scaling parameter that accounts for the target reflectivity as well as the propagation effects in the $k$th receive channel, $n_k$ is the propagation delay of the target returns accounting for both the distance between the IO and the target and the distance between the target and the $k$th receive platform, $\Omega_k$ is the normalized Doppler frequency in the $k$th receive channel, and $w_k(n)$ is the Gaussian noise with zero mean and variance $\sigma^2$, i.e., $w_k(n) \sim \mathcal{CN}0, \sigma^2)$.

Suppose that $w_k(n)$ for $n = 1, 2, \ldots, N$ and $k = 1, 2, \ldots, K$ are identically and independently distributed (i.i.d.).

It is worth noting that the time delays (or frequency shifts) in the different channels may be distinct due to the geographical dispersion of the receivers. In practice, a set of time delay and frequency shift (e.g., $(n_1, \Omega_1)$) in one of the received channels is selected as a reference set. Notice that the differences in the time delay (or frequency shift) between different received signals, instead of the original time delays (or frequency shifts) in all received signals, are of interest. These differences $(\breve{n}_k, \breve{\Omega}_k)$, where $\breve{n}_k = n_k - n_1$ and $\breve{\Omega}_k = \Omega_k - \Omega_1$, can be obtained by a cross-correlation operation between $x_k(n)$ and $x_1(n)$ [17]. Therefore, for a specific reference set $(n_1, \Omega_1)$, we can compensate for the time delays and Doppler shifts of the received signals in all other channels. A similar compensation operation can be found in [1] and [37]. In addition, although the time delay $n_1$ and the Doppler shift $\Omega_1$ in the reference set are not known *a priori*, their estimates can be obtained using a grid search as in conventional active radars [38].

Let the null hypothesis $(H_0)$ be such that the received data are free of the target echoes and the alternative hypothesis $(H_1)$ be such that the received data contain the target echoes. After compensating for a particular hypothesized set, the passive detection problem can be formulated in terms of the following binary hypothesis test

$$\begin{cases} H_0 : \mathbf{x}_k = \mathbf{w}_k \\ H_1 : \mathbf{x}_k = \alpha_k \mathbf{s} + \mathbf{w}_k \end{cases} \quad k = 1, 2, \ldots, K, \tag{2}$$

where

- $\mathbf{x}_k$ denotes the $N \times 1$ sample vector in the $k$th receiver ($N$ is the number of samples);
- $\mathbf{s}$ is an $N \times 1$ sample vector, whose elements are unknown due to the non-cooperative nature of the IO;
- $\alpha_k$ is an unknown scaling parameter that accounts for the channel propagation effect and the target reflectivity;
- $\mathbf{w}_k$ is an $N \times 1$ noise vector in the $k$th receiver; they are modeled as independent circular complex Gaussian processes with zero mean and covariance matrix $\sigma^2 \mathbf{I}_N$, where $\sigma^2$ denotes the noise power, i.e., $\mathbf{w}_k \sim \mathcal{CN}(\mathbf{0}, \sigma^2 \mathbf{I}_N)$.

In practice, a long integration time is usually required in the passive detection due to the weakness of the target returns. Hence, we impose an assumption that $N > K$ in the passive detection problem (2).

## III. GLRT Detection With Unknown Noise Power

In this section, we consider the design of a GLRT detector for the case of unknown noise power. According to the Neyman-Pearson criterion, the optimum solution to the above hypothesis testing problem (2) is obtained by comparing the ratio of the likelihood of the received data under hypothesis $H_1$ over that under hypothesis $H_0$ with an appropriate detection threshold. However, the optimum detector cannot be used since these likelihood functions depend on the unknown parameters $\mathbf{s}$, $\alpha_k$, and $\sigma^2$.

### A. GLRT Detector With Unknown $\sigma^2$

To obtain a practical detector, we resort to the GLRT, which is equivalent to replacing all the unknown parameters with their maximum likelihood estimates (MLEs) [39]. In other words, the GLRT detector in this case is to be obtained from

$$\frac{\max_{\{\alpha_k, \mathbf{s}, \sigma^2\}} f(\mathbf{X}|H_1)}{\max_{\{\sigma^2\}} f(\mathbf{X}|H_0)} \underset{H_0}{\overset{H_1}{\gtrless}} \xi, \tag{3}$$

where $\xi$ is the detection threshold,

$$\mathbf{X} = [\mathbf{x}_1, \mathbf{x}_2, \ldots, \mathbf{x}_K], \tag{4}$$

$f(\mathbf{X}|H_1)$ and $f(\mathbf{X}|H_0)$ are the probability density functions (PDFs) of the received signals under $H_1$ and $H_0$, respectively, i.e.,

$$f(\mathbf{X}|H_1) = \frac{1}{\pi^{KN} \sigma^{2KN}} \exp\left( -\frac{1}{\sigma^2} \sum_{k=1}^{K} \|\mathbf{x}_k - \alpha_k \mathbf{s}\|^2 \right), \tag{5}$$

and

$$f(\mathbf{X}|H_0) = \frac{1}{\pi^{KN} \sigma^{2KN}} \exp\left( -\frac{1}{\sigma^2} \sum_{k=1}^{K} \|\mathbf{x}_k\|^2 \right). \tag{6}$$

It can be shown that the MLE of $\alpha_k$ under $H_1$ is [1, eq. (5)]

$$\hat{\alpha}_k = \frac{\mathbf{s}^\dagger \mathbf{x}_k}{\mathbf{s}^\dagger \mathbf{s}}. \tag{7}$$

Inserting this MLE of $\alpha_k$ into (5) leads to

$$\max_{\{\alpha_k\}} f(\mathbf{X}|H_1) = \frac{1}{\pi^{KN} \sigma^{2KN}} \times \exp\left[ -\frac{1}{\sigma^2} \left( \sum_{k=1}^{K} \|\mathbf{x}_k\|^2 - \frac{\mathbf{s}^\dagger \mathbf{X}\mathbf{X}^\dagger \mathbf{s}}{\mathbf{s}^\dagger \mathbf{s}} \right) \right]. \tag{8}$$

The maximization of (8) with respect to $\mathbf{s}$ is equivalent to maximizing the Rayleigh quotient $\frac{\mathbf{s}^\dagger \mathbf{X}\mathbf{X}^\dagger \mathbf{s}}{\mathbf{s}^\dagger \mathbf{s}}$. This maximum value is exactly the largest eigenvalue of $\mathbf{X}\mathbf{X}^\dagger$, i.e.,

$$\max_{\{\mathbf{s}\}} \frac{\mathbf{s}^\dagger \mathbf{X}\mathbf{X}^\dagger \mathbf{s}}{\mathbf{s}^\dagger \mathbf{s}} = \lambda_1(\mathbf{X}\mathbf{X}^\dagger) = \lambda_1(\mathbf{\Phi}), \tag{9}$$

where

$$\mathbf{\Phi} = \mathbf{X}^\dagger \mathbf{X}. \tag{10}$$

It is worth noting that the employment of the $K$-dimensional matrix $\mathbf{\Phi}$ instead of the $N$-dimensional matrix $\mathbf{X}\mathbf{X}^\dagger$ in (9) is more computationally effective in calculating the maximum eigenvalue. In addition, it should be pointed out that there exists an ambiguity in the estimation of the norm of the vector $\mathbf{s}$. It means that $\|\mathbf{s}\|$ cannot be uniquely determined. Nevertheless, this ambiguity does not affect the GLRT.

Substituting (9) into (8) produces

$$\max_{\{\alpha_k, \mathbf{s}\}} f(\mathbf{X}|H_1) = \frac{1}{\pi^{KN} \sigma^{2KN}} \times \exp\left[ -\frac{1}{\sigma^2} \left( \sum_{k=1}^{K} \|\mathbf{x}_k\|^2 - \lambda_1(\mathbf{\Phi}) \right) \right]. \tag{11}$$

It is easy to show that the MLE of the noise power under $H_1$ is

$$\hat{\sigma}^2 = \frac{1}{KN} \left( \sum_{k=1}^{K} \|\mathbf{x}_k\|^2 - \lambda_1(\mathbf{\Phi}) \right). \tag{12}$$

Substituting (12) into (11) yields

$$\max_{\{\alpha_k,\mathbf{s},\sigma^2\}} f(\mathbf{X}|H_1) = \left[\frac{e\pi}{KN}\left(\sum_{k=1}^{K}\|\mathbf{x}_k\|^2 - \lambda_1(\mathbf{\Phi})\right)\right]^{-KN}. \tag{13}$$

According to (6), we obtain the MLE of the noise power under $H_0$ to be

$$\hat{\sigma}^2 = \frac{1}{KN}\sum_{k=1}^{K}\|\mathbf{x}_k\|^2. \tag{14}$$

Inserting (14) into (6), we have

$$\max_{\{\sigma^2\}} f(\mathbf{X}|H_0) = \left[\frac{e\pi}{KN}\sum_{k=1}^{K}\|\mathbf{x}_k\|^2\right]^{-KN}. \tag{15}$$

Applying (13) and (15) to (3) and making an equivalent transformation, we derive the GLRT detector as

$$\Xi = \frac{\lambda_1(\mathbf{\Phi})}{\sum_{k=1}^{K}\lambda_k(\mathbf{\Phi})} \underset{H_0}{\overset{H_1}{\gtrless}} \xi, \tag{16}$$

where $\xi$ is a suitable modified version of the threshold in (3). Note that in the equivalent transformation in (16) we have used the result

$$\sum_{k=1}^{K}\lambda_k(\mathbf{\Phi}) = \mathrm{tr}(\mathbf{\Phi}) = \sum_{k=1}^{K}\|\mathbf{x}_k\|^2. \tag{17}$$

In the particular case where $K = 2$, the eigenvalues of $\mathbf{\Phi}$ can be explicitly expressed as elementary functions of the received signals. More precisely, $\mathbf{\Phi}$ in (10) for $K = 2$ can be written as

$$\mathbf{\Phi} = \begin{bmatrix} \|\mathbf{x}_1\|^2 & \mathbf{x}_1^\dagger\mathbf{x}_2 \\ \mathbf{x}_2^\dagger\mathbf{x}_1 & \|\mathbf{x}_1\|^2 \end{bmatrix}. \tag{18}$$

It is easy to show that the largest and smallest eigenvalues are,

$$\lambda_1(\mathbf{\Phi}) = \frac{\|\mathbf{x}_1\|^2+\|\mathbf{x}_2\|^2+\sqrt{\left(\|\mathbf{x}_1\|^2-\|\mathbf{x}_2\|^2\right)^2+4\left|\mathbf{x}_1^\dagger\mathbf{x}_2\right|^2}}{2}, \tag{19}$$

and

$$\lambda_2(\mathbf{\Phi}) = \frac{\|\mathbf{x}_1\|^2+\|\mathbf{x}_2\|^2-\sqrt{\left(\|\mathbf{x}_1\|^2-\|\mathbf{x}_2\|^2\right)^2+4\left|\mathbf{x}_1^\dagger\mathbf{x}_2\right|^2}}{2}, \tag{20}$$

respectively. As a result, the test statistic $\Xi$ in (16) for $K = 2$ can be explicitly written as the following equivalent form:

$$\tilde{\Xi} = \frac{\|\mathbf{x}_1\|^2+\|\mathbf{x}_2\|^2+\sqrt{\left(\|\mathbf{x}_1\|^2-\|\mathbf{x}_2\|^2\right)^2+4\left|\mathbf{x}_1^\dagger\mathbf{x}_2\right|^2}}{\|\mathbf{x}_1\|^2+\|\mathbf{x}_2\|^2} \underset{H_0}{\overset{H_1}{\gtrless}} \tilde{\xi}, \tag{21}$$

where $\tilde{\xi} = 2\xi$.

For the purpose of having a deeper insight into the structure of the proposed GLRT detector, we equivalently write (16) as

$$\frac{1}{\frac{1}{KN}\sum_{k=2}^{K}\lambda_k(\mathbf{\Phi})}\lambda_1(\mathbf{\Phi}) \underset{H_0}{\overset{H_1}{\gtrless}} \bar{\xi}, \tag{22}$$

where $\bar{\xi}$ is a suitable modified version of the threshold in (16). Interestingly, it can be seen from (12) and (17) that the MLE of the noise power under $H_1$ is

$$\hat{\sigma}^2 = \frac{1}{KN}\sum_{k=2}^{K}\lambda_k(\mathbf{\Phi}), \tag{23}$$

which is exactly the denominator of the test statistic in (22). This is to say, the test statistic in (22) can be interpreted as the maximum eigenvalue normalized by the estimated noise power.

### *B. Performance Analysis*

In order to complete the construction of the test in (16), we should provide an approach to set the detection threshold. To this end, a closed-form expression for the probability of false alarm of the GLRT detector in (16) is derived, which can be employed to compute the detection threshold for any given probability of false alarm. According to [40], the probability of false alarm of the GLRT detector in (16) can be expressed as

$$\begin{aligned} P_{\mathrm{FA}} =& 1 - \Gamma(KN)M_0^{-1}\sum_{k=1}^{K}\sum_{j=N-K}^{(N+K-2k)k} \\ &\times \sum_{i=0}^{KN-j-2}\frac{\beta_{k,j}\mathrm{C}_{KN-j-2}^{i}(-k)^i}{\Gamma(KN-j-1)} \\ &\times \left\{ g_1(\xi,j,i)\left[u\left(\xi-\frac{1}{K}\right)-u\left(\xi-\frac{1}{k}\right)\right] \right. \\ &\left. + g_2(k,j,i)u\left(\xi-\frac{1}{k}\right)\right\}, \end{aligned} \tag{24}$$

where $\frac{1}{K} \le \xi \le 1$,

$$M_0 = \prod_{k=1}^{K}\left[(K-k)!(N-k)!\right], \tag{25}$$

$$g_1(\xi,j,i) = \frac{1}{j+i+1}\left[\xi^{j+i+1} - K^{-(j+i+1)}\right], \tag{26}$$

and

$$g_2(k,j,i) = \frac{1}{j+i+1}\left[k^{-(j+i+1)} - K^{-(j+i+1)}\right]. \tag{27}$$

Note that the coefficients $\beta_{k,j}$ in (24) can be obtained by the following equality [41]:

$$\frac{\mathrm{d}}{\mathrm{d}\xi}\det\{\mathbf{\Theta}(\xi)\} = \sum_{k=1}^{K}\sum_{j=N-K}^{(N+K-2k)k}\beta_{k,j}\xi^j\exp(-k\xi), \tag{28}$$

where the $(n,m)$th entry of $\mathbf{\Theta}$ is given by

$$\mathbf{\Theta}_{n,m}(\xi) = \gamma(N-K+n+m-1,\xi), \tag{29}$$

with the lower incomplete Gamma function $\gamma(n,x)$ defined as

$$\gamma(n,y) = \int_0^y t^{n-1}\exp(-t)\mathrm{d}t. \tag{30}$$

It is easy to determine $\beta_{k,j}$ in (28) by using most symbolic softwares such as Maple and Matlab (see [42, Algorithm 1]).

In the particular case where $K=2$, the probability of false alarm of the GLRT detector in (21) can be explicitly written in terms of elementary functions, i.e.,

$$P_{\mathrm{FA}} = 1 - \frac{\Gamma(2N)}{\Gamma(N)\Gamma(N-1)}\left[h(\xi)-h(0.5)\right], \tag{31}$$

where $\frac{1}{2} \le \xi \le 1$, and

$$h(y) = \sum_{k=0}^{N-2} \mathrm{C}_{N-2}^{k}(-1)^{N-2-k} \times \left(\frac{y^{2N-k-3}}{2N-k-3} - 4\frac{y^{2N-k-2}}{2N-k-2} + 4\frac{y^{2N-k-1}}{2N-k-1}\right). \tag{32}$$

It can be seen from (24) that the probability of false alarm of the GLRT detection in (16) is independent of the noise power. It implies that the GLRT detection in (16) possesses the desirable CFAR property against the noise power.

As to the detection performance, unfortunately, a closed-form expression for the detection probability of the GLRT detector in (16) is intractable.

## IV. Detection With Known Noise Power

Now, we turn to the case of known noise power. The GCC has been proposed in [1], [2] to handle the passive detection problem in this case, which can be expressed as

$$\Delta = \lambda_1(\mathbf{\Phi}) \underset{H_0}{\overset{H_1}{\gtrless}} \delta, \tag{33}$$

where $\delta$ is the detection threshold. Using (19), we can equivalently write the GCC detector in (33) for $K=2$ as

$$\tilde{\Delta} = \|\mathbf{x}_1\|^2 + \|\mathbf{x}_2\|^2 + \sqrt{\left(\|\mathbf{x}_1\|^2 - \|\mathbf{x}_2\|^2\right)^2 + 4\left|\mathbf{x}_1^{\dagger}\mathbf{x}_2\right|^2} \underset{H_0}{\overset{H_1}{\gtrless}} \tilde{\delta}, \tag{34}$$

where $\tilde{\delta} = 2\delta$.

Since the noise power $\sigma^2$ is assumed known, we can equivalently write (33) as

$$\Delta_1 = \frac{1}{\sigma^2}\lambda_1(\mathbf{\Phi}) \underset{H_0}{\overset{H_1}{\gtrless}} \delta_1, \tag{35}$$

where $\delta_1 = \frac{\delta}{\sigma^2}$. Comparison between the test statistics in (22) and (35) reveals that both test statistics are the normalized maximum eigenvalue of $\mathbf{\Phi}$, and the normalization factors used in (22) and (35) are the estimated and exact noise powers, respectively.

It should be pointed out that the performance analysis of the GCC detector is not provided in [1], [2]. In the following, we fill this gap by offering closed-form expressions for the probabilities of false alarm and detection.

Recall that $\mathbf{\Phi} = \mathbf{X}^{\dagger}\mathbf{X}$ where $\mathbf{X} = [\mathbf{x}_1, \mathbf{x}_2, \ldots, \mathbf{x}_K]$. Due to the Gaussian properties of $\mathbf{x}_k$ for $k = 1,2,\ldots,K$, we can obtain that $\mathbf{\Phi}$ has a complex Wishart distribution under $H_0$, i.e., $\mathbf{\Phi} \sim \mathcal{W}_K(N, \sigma^2\mathbf{I}_K)$. Note that the cumulative distribution function (CDF) of the largest eigenvalue of a central Wishart matrix has been derived in [43]. Based on this result, we can obtain the probability of false alarm of the GCC detector in (33) to be

$$P_{\mathrm{FA}} = 1 - \frac{\det\{\mathbf{\Psi}(\delta)\}}{\sigma^{2KN}\prod_{k=1}^{K}\left[\Gamma(N-k+1)\Gamma(K-k+1)\right]}, \tag{36}$$

where the $(i,j)$th element of the $K\times K$ matrix $\mathbf{\Psi}$ is given by

$$\mathbf{\Psi}_{i,j}(\delta) = \sigma^{2(N-K+i+j-1)}\gamma\left(N-K+i+j-1, \frac{\delta}{\sigma^2}\right). \tag{37}$$

In addition, the detection probability of the GLRT detector in (33) can be written as [44]

$$P_{\mathrm{D}} = 1 - \frac{\exp\left(-\frac{\theta}{\sigma^2}\right)\det\{\mathbf{\Omega}(\delta)\}}{\sigma^{2(KN-2K+2)}\theta^{K-1}\Gamma(N-K-1)M_1}, \tag{38}$$

where $\theta$ is the non-zero eigenvalue of the matrix $\|\mathbf{s}\|^2\boldsymbol{\alpha}\boldsymbol{\alpha}^{\dagger}$ with $\boldsymbol{\alpha} = [\alpha_1,\ldots,\alpha_K]^T$,

$$M_1 = \prod_{k=1}^{K-1}\left[\Gamma(N-k)\Gamma(K-k)\right], \tag{39}$$

and the entries of the $K\times K$ matrix $\mathbf{\Omega}$ are given in Appendix A.

## V. Simulations Results

In this section, numerical simulations are conducted to validate the above theoretical analysis and illustrate the performance of the proposed detector. The signal $\mathbf{s}$ transmitted from the IO is sampled from $\mathcal{CN}(\mathbf{0},\mathbf{I})$. The signal-to-noise ratio (SNR) is defined by

$$\mathrm{SNR} = 10\log_{10}\frac{\frac{1}{KN}\sum_{k=1}^{K}\left(|\alpha_k|^2\sum_{n=1}^{N}|s(n)|^2\right)}{\sigma^2}. \tag{40}$$

For comparison purposes, the GC detector and the ED are introduced. The GC detector can be represented as [34]

$$\Lambda_{\mathrm{GC}} = 1 - \frac{\det\{\mathbf{\Phi}\}}{\prod_{k=1}^{K}\|\mathbf{x}_k\|^2} \underset{H_0}{\overset{H_1}{\gtrless}} \zeta_{\mathrm{GC}}, \tag{41}$$

where $\zeta_{\mathrm{GC}}$ is the detection threshold. The ED detector can be expressed as

$$\Lambda_{\mathrm{ED}} = \sum_{k=1}^{K}\|\mathbf{x}_k\|^2 \underset{H_0}{\overset{H_1}{\gtrless}} \zeta_{\mathrm{ED}}, \tag{42}$$

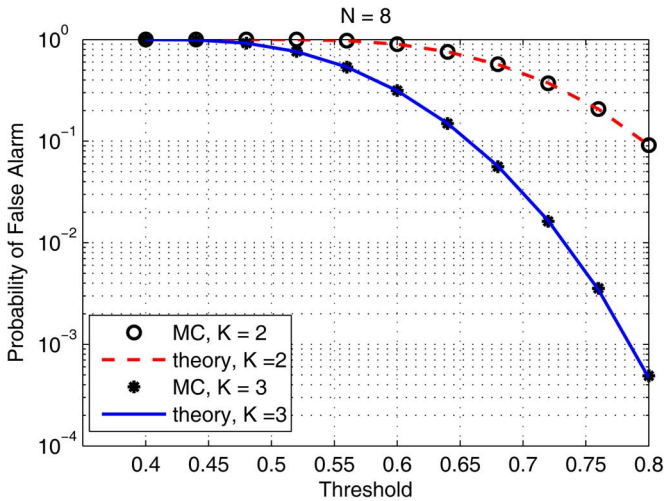


Fig. 2. Probability of false alarm of the GLRT detector in (16) versus the detection threshold for $N = 8$. The dashed and solid lines denote the results obtained with (31) and (24) for $K = 2$ and $K = 3$, respectively. The symbols "$\circ$" and "$*$" denote the results obtained using MC simulations for $K = 2$ and $K = 3$, respectively.

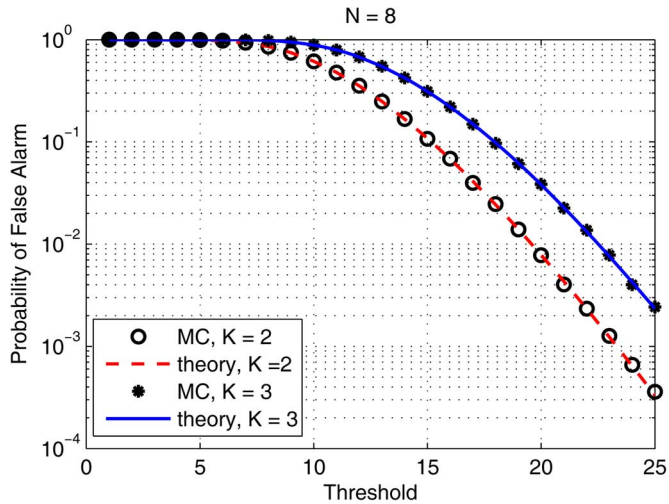


Fig. 3. Probability of false alarm of the GCC detector in (33) versus the detection threshold for $N = 8$. The dashed and solid lines denote the results obtained with (36) for $K = 2$ and $K = 3$, respectively. The symbols "$\circ$" and "$*$" denote the results obtained using MC simulations for $K = 2$ and $K = 3$, respectively.

where $\zeta_{\mathrm{ED}}$ is the detection threshold. The probabilities of false alarm and detection of the GC detector can be seen in [34], [35]. For convenience of performance evaluation, the probabilities of false alarm and detection of the ED are derived in Appendix B. Obviously, the expression in (B.4) for the false alarm rate is related to the noise power, which implies that the ED does not possess a CFAR property against the noise power.

### *A. False Alarm Rates*

The probability of false alarm of the proposed GLRT detector in (16) as a function of the detection threshold is presented in Fig. 2, where $N = 8$ and $\sigma^2 = 1$. The dashed and solid lines denote the results obtained with (31) and (24) derived in Section III-B for $K = 2$ and $K = 3$, respectively. The symbols "$\circ$" and "$*$" denote the results obtained using Monte Carlo (MC) simulations for $K = 2$ and $K = 3$, respectively. The number of independent trials used to calculate the probability of false alarm in each case is $10^5$. It can be seen that there is exact agreement between the theoretical results and the simulation results.

In Fig. 3, we plot the probability of false alarm of the GCC in (33) as a function of the detection threshold. The results obtained by the theoretical expression in (36) and the MC techniques are all provided. The parameters used in Fig. 3 are the same as those in Fig. 2. It can be observed that the theoretical results match the MC results pretty well.

### *B. Detection Performance Without Uncertainty in Noise Power*

The detection probability curves of the GCC detector in (33) and the proposed GLRT detector in (16) as a function of the number of samples $N$ are plotted in Fig. 4, where $\mathrm{SNR} = -5$ dB and $P_{\mathrm{FA}} = 0.01$. Both the theoretical expression in (38) and the MC simulation are used to obtain the detection probability of the GCC detector in (33). The theoretical result and the MC result are denoted by the solid line and the symbol "$\circ$", respectively. It is shown that they are consistent with each other.

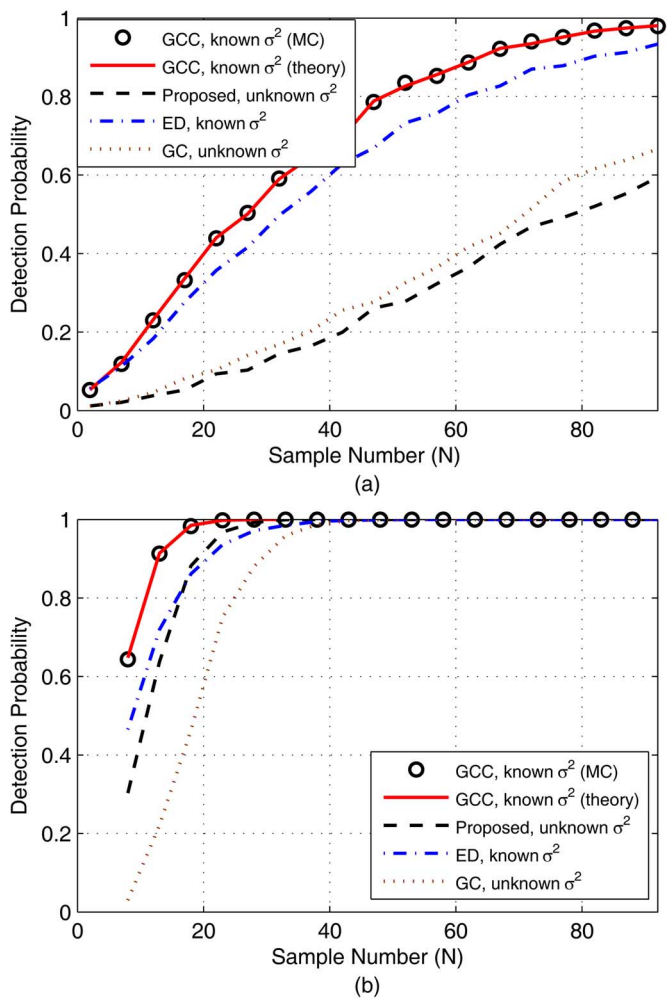


Fig. 4. Performance comparisons with $\mathrm{SNR} = -5$ dB for different $N$. (a) $\mathrm{K} = 2$; (b) $\mathrm{K} = 8$.

For comparison purposes, the detection probabilities of both the GC detector and the ED are also provided. It should be pointed out that the detection probability curves of the proposed

GLRT detector in (16) and the GC detector in (41) are plotted using MC simulations, and the curve of the ED is obtained with the theoretical expression in (B.5). The number of independent trials used to calculate the detection probability in each case is $10^4$.

From Fig. 4(a) with $K = 2$, we can observe that the GCC detector in (33) developed with known noise power performs the best, the ED has slightly inferior performance, the GC detector provides a detection performance obviously worse than the ED, and the GLRT detector in (16) proposed with unknown noise power performs the worst. Obviously, the GCC detector in (33) outperforms the proposed GLRT detector in (16) and the GC detector, due to the exploitation of *a priori* knowledge about the noise power. In addition, the GCC detector in (33) provides a detection performance better than the ED, since it exploits the coherence between the received signals.

In Fig. 4(b) with $K = 8$, it is shown that the GLRT detector in (16) proposed with unknown noise power has better performance than the GC detector, and even outperforms the ED in the large sample region (e.g., $N = 18$ in this example). However, the performance of the GLRT detector in (16) proposed for unknown noise power is worse than that of the GCC detector in (33) developed for known noise power.

Fig. 4 reveals that the increase in the sample number leads to a gain in the detection performance of all the detectors considered here. In addition, it is found that the GC detector outperforms the proposed GLRT detector in (16) when the number of sensors is small (e.g., $K = 2$ in Fig. 4(a)). When the number of sensors increases up to 8, as shown in Fig. 4(b), the proposed GLRT detector in (16) significantly outperforms the GC detector.

In order to clarify the effect of $K$ on the performance of all the detectors considered, we plot the detection probability as a function of $K$ in Fig. 5, where $N = 30$, $\mathrm{SNR} = -5$ dB and $P_{\mathrm{FA}} = 0.01$. It is demonstrated that performance improves with increased number of sensors. More importantly, the proposed GLRT detector in (16) performs better than the GC detector, when multiple receivers (more than 3) are used. Additionally, the proposed GLRT detector in (16) also outperforms the ED, when the number of the receivers is large (e.g., $K \geq 6$ in this example).

### C. Detection Performance With Uncertainty in Noise Power

Note that the noise power is required to be exactly known to obtain the detection thresholds of the GCC detector in (33) and the ED in (42). In practice, the noise power is usually unknown and need to be estimated. Nevertheless, the estimation of the noise power leads to an error. Denote the estimated noise power by $\tilde{\sigma}^2 = \epsilon\sigma^2$, where $\epsilon$ describes how accurate the estimate is. Using the estimated noise power to set the detection thresholds, (33) and (42) become, respectively,

$$\Delta_{\mathrm{GCC-U}} = \lambda_1(\mathbf{\Phi}) \underset{H_0}{\overset{H_1}{\gtrless}} \delta_{\mathrm{GCC-U}}, \tag{43}$$

and

$$\Lambda_{\mathrm{ED-U}} = \sum_{k=1}^{K} \|\mathbf{x}_k\|^2 \underset{H_0}{\overset{H_1}{\gtrless}} \zeta_{\mathrm{ED-U}}. \tag{44}$$

Note that $\delta_{\mathrm{GCC-U}}$ and $\zeta_{\mathrm{ED-U}}$ can be obtained by replacing $\sigma^2$ with $\tilde{\sigma}^2$ in (36) and (B.4), respectively. For ease of notation, the detectors in (43) and (44) are referred to as GCC-U and ED-U, respectively.

In the following, we examine the effect of the uncertainty in the noise power on the detection performance of the GCC-U

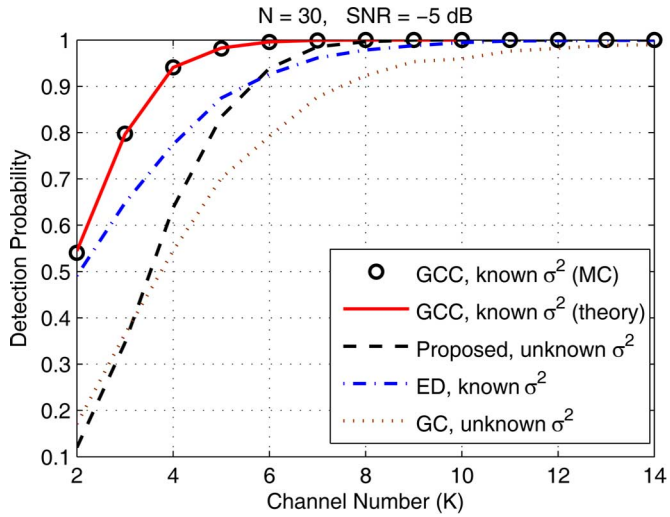


Fig. 5. Performance comparisons with $N = 30$ for different $K$.

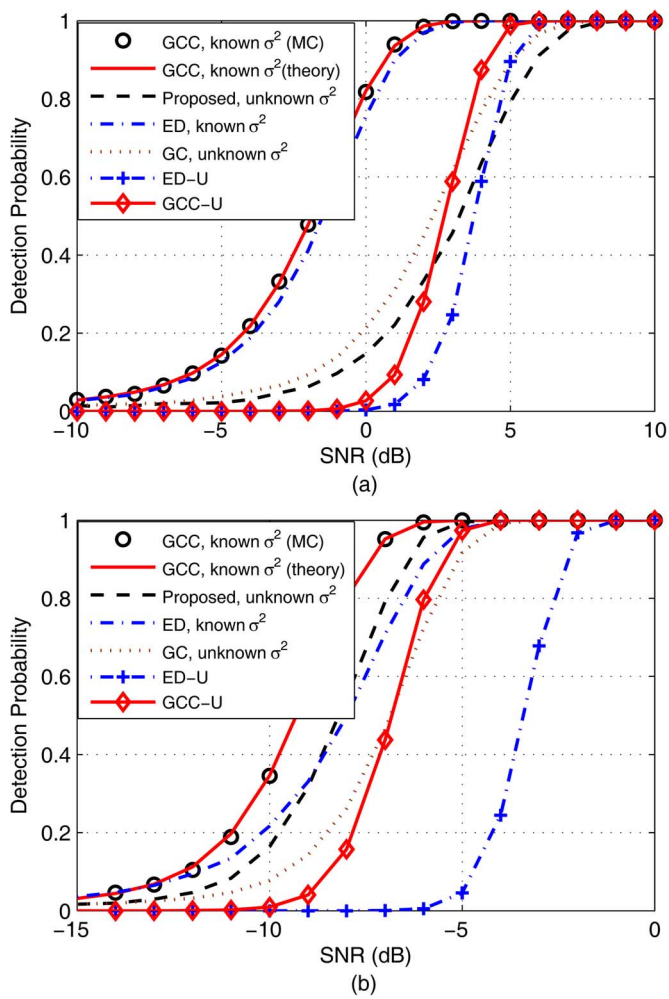


Fig. 6. Performance comparisons with uncertainty in the noise power. (a) $\mathrm{K} = 2, \mathrm{N} = 8, \mathrm{U} = 3$ dB; (b) $\mathrm{K} = 8, \mathrm{N} = 30, \mathrm{U} = 1$ dB.

detector in (43) and the ED-U in (44). The noise uncertainty factor is defined as $U = 10\log_{10}\epsilon$.

In Fig. 6(a), the detection performance of the GCC-U detector in (43) and the ED-U in (44) versus SNR for the case of $U = 3$ dB is presented. Here, we select $K = 2$, $N = 8$, and $P_{\rm FA} = 0.01$. It can be seen that the GCC detector and the ED, both of which are derived with known noise power, do not always outperform the proposed GLRT detector in (16), when there is 3 dB uncertainty in the estimated noise power.

Fig. 6(b) plots the detection probability as a function of SNR for $K = 8$, $N = 30$ and $U = 1$ dB. Other parameters are selected the same as those in Fig. 6(a). We observe that the GLRT detector in (16) proposed with unknown noise power for large $N$ and $K$ has an obvious gain in the detection performance with respect to both the GCC detector and the ED, when there is only 1 dB uncertainty in the estimated noise power. It implies that the performance of the GCC detector in (33) and the ED for the case of large $K$ and $N$ is very sensitive to the uncertainty in the noise power estimate.

## VI. Conclusion

We examined the problem of passive detection with a multistatic radar system consisting of a non-cooperative IO and multiple geographically distributed receive platforms. Due to the non-cooperative nature of the IO, the signal transmitted from the IO is unknown. A GLRT detector is proposed for the case in which both the transmitted signal and the noise power are unknown. It has the form of the ratio of the maximum eigenvalue to the sum of all eigenvalues of the Gram matrix or covariance matrix of the received signals. The proposed GLRT detector can also be transformed as an equivalent form of the maximum eigenvalue of the Gram matrix normalized by the estimated noise power. The probability of false alarm of the proposed GLRT detector is derived, implying that the proposed GLRT detector possesses the desirable CFAR property against the noise power. Notice that this expression can be used to set the detection threshold for a preassigned false alarm rate. In addition, we employ the GCC detector developed in [1], [2] to deal with the passive detection problem in the case of known noise power. The performance of the GCC detector with known poise power is evaluated in terms of the probabilities of false alarm and detection. All analytical results derived in this study are verified using MC simulations. Simulation results demonstrate that the performance of the proposed GLRT detector increases as the number of receive platforms or/and data samples increases. In particular, when the number of receive platforms is large, the proposed GLRT detector outperforms the ED and the GC detector. Note that, the GCC detector developed with known noise power in [1], [2] performs the best due to its usage of *a priori* knowledge on the noise power and the coherence between the received signals. However, it performed worse than the proposed GLRT detector with unknown noise power, when uncertainty in the noise power exists.

## Appendix A
## Elements of $\mathbf{\Omega}$

The $(i,j)$th element of the $K\times K$ matrix $\mathbf{\Omega}$ for $j\neq 1$ is given by

$$\mathbf{\Omega}_{i,j}(\delta) = \sigma^{2(N+K-i-j+1)}\gamma\left(N+K-i-j+1, \frac{\delta}{\sigma^2}\right), \quad \text{(A.1)}$$

and the $(i,1)$th element of $\mathbf{\Omega}$ is expressed as

$$\mathbf{\Omega}_{i,1}(\delta) = \int_0^{\delta} t^{N-i}\exp\left(-\frac{t}{\sigma^2}\right){}_0F_1\left(N-K+1;\frac{\theta t}{\sigma^4}\right)\mathrm{d}t, \quad \text{(A.2)}$$

with ${}_0F_1(n;y)$ denoting the hypergeometric function of Bessel type, i.e.,

$${}_0F_1(n;y) = \sum_{k=0}^{\infty}\frac{y^k}{(n)_k k!}. \quad \text{(A.3)}$$

Using the change of variable $y = \frac{t}{\sigma^2}$, the integral in (A.2) can be written as

$$\mathbf{\Omega}_{i,1}(\delta) = \sigma^{2(N-i+1)}J_i(\delta), \quad \text{(A.4)}$$

where

$$J_i(\delta) = \int_0^{\frac{\delta}{\sigma^2}} y^{N-i}\exp(-y)\,{}_0F_1\left(N-K+1;\frac{\theta}{\sigma^2}y\right)\mathrm{d}y. \quad \text{(A.5)}$$

Furthermore, the integral in (A.5) can be cast into

$$J_i(\delta) = \Gamma(N-i+1){}_1F_1\left(N-i+1;L+1;\frac{\theta}{\sigma^2}\right) - \frac{\Gamma(L+1)}{2^{q_i}a^L}\exp\left(\frac{\theta}{\sigma^2}\right)Q_{L+2q_i+1,L}(a,b), \quad \text{(A.6)}$$

where $L = N-K$, $q_i = K-i$, $a = \sqrt{\frac{2\theta}{\sigma^2}}$, $b = \sqrt{\frac{2\delta}{\sigma^2}}$, ${}_1F_1(n;m;y)$ is the confluent hypergeometric function given as

$${}_1F_1(n;m;y) = \sum_{k=0}^{\infty}\frac{(n)_k}{(m)_k k!}y^k, \quad \text{(A.7)}$$

and $Q_{n,m}(x,y)$ is the Nuttall $Q$-function defined as [45]

$$Q_{n,m}(y,z) = \int_z^{\infty} t^n\exp\left(-\frac{t^2+y^2}{2}\right)I_m(yt)\mathrm{d}t, \quad \text{(A.8)}$$

with $I_m$ denoting the $n$th order modified Bessel function of the first kind. According to [46, eq. (8)], the Nuttall $Q$-function in (A.6) can be expressed as

$$Q_{L+2q_i+1,L}(a,b) = \sum_{l=1}^{q_i+1}D_l(q_i)a^{L+2(l-1)}Q_{L+l}(a,b) + \exp\left(-\frac{a^2+b^2}{2}\right)\sum_{l=1}^{q_i}T_{q_i,l}(b^2) \times a^{l-1}b^{L+l+1}I_{L+l-1}(ab), \quad \text{(A.9)}$$

where

$$D_l(q_i) = \frac{q_i!}{(l-1)!}2^{q_i-l+1}\mathrm{C}_{q_i+L}^{q_i-l+1}, \quad \text{(A.10)}$$

$$T_{q_i,l}(b^2) = \sum_{j=0}^{q_i-l}\frac{(q_i-1-j)!}{(l-1)!}2^{q_i-l-j}\mathrm{C}_{q_i+L}^{q_i-l-j}b^{2j}, \quad \text{(A.11)}$$

and $Q_n(y,z)$ is the $n$th order generalized Marcum $Q$-function defined as [47]

$$Q_n(y,z)=\frac{1}{y^{n-1}}\int_z^\infty t^n\exp\left(-\frac{t^2+y^2}{2}\right)I_{n-1}(yt)\mathrm{d}t. \quad \text{(A.12)}$$

## Appendix B
## Performance Analysis of ED

According to (2), we have

$$\begin{cases}\mathbf{x}_k\sim\mathcal{CN}(\mathbf{0},\sigma^2\mathbf{I}_N), & \text{under } H_0,\\ \mathbf{x}_k\sim\mathcal{CN}(\alpha_k\mathbf{s},\sigma^2\mathbf{I}_N), & \text{under } H_1,\end{cases} \quad \text{(B.1)}$$

where $k=1,2,\ldots,K$. Under $H_0$, $\Lambda_{\mathrm{ED}}$ in (42) is the sum of the square of $K$ i.i.d. complex Gaussian vectors with zero mean and covariance matrix $\sigma^2\mathbf{I}_N$. Under $H_1$, $\Lambda_{\mathrm{ED}}$ in (42) is the sum of the square of $K$ complex Gaussian vectors where the $k$th Gaussian vector has mean $\alpha_k\mathbf{s}$ and covariance matrix $\sigma^2\mathbf{I}_N$. As a consequence,

$$\begin{cases}\Lambda_{\mathrm{ED}}=\sum_{k=1}^K\|\mathbf{x}_k\|^2\sim\frac{\sigma^2}{2}\chi^2_{2KN}, & \text{under } H_0,\\ \Lambda_{\mathrm{ED}}=\sum_{k=1}^K\|\mathbf{x}_k\|^2\sim\frac{\sigma^2}{2}\chi'^2_{2KN}(2\rho), & \text{under } H_1,\end{cases} \quad \text{(B.2)}$$

where $\chi^2_n$ and $\chi'^2_n$ denote the central and non-central Chi-squared distributions, respectively, and the non-central parameter $\rho$ is given by

$$\rho=\frac{|\mathbf{s}|^2|\boldsymbol{\alpha}|^2}{\sigma^2}. \quad \text{(B.3)}$$

Therefore, the probability of false alarm of the ED in (42) can be expressed as

$$\begin{aligned}P_{\mathrm{FA}}&=\int_\zeta^\infty f(\Lambda|H_0)\mathrm{d}\Lambda\\&=\frac{1}{\Gamma(KN)}\int_{\frac{\zeta}{\sigma^2}}^\infty t^{KN-1}\exp(-t)\mathrm{d}t\\&=1-\frac{1}{\Gamma(KN)}\gamma\left(KN,\frac{\zeta}{\sigma^2}\right),\end{aligned} \quad \text{(B.4)}$$

where the lower incomplete Gamma function $\gamma(n,y)$ is defined in (30). Furthermore, the detection probability of the ED in (44) can be calculated as

$$\begin{aligned}P_{\mathrm{D}}&=\int_\zeta^\infty f(\Lambda|H_1)\mathrm{d}\Lambda\\&=\int_{\frac{\zeta}{\sigma^2}}^\infty\left(\frac{t}{\rho}\right)^{\frac{KN-1}{2}}\exp\left[-(t+\rho)\right]I_{KN-1}(\sqrt{\rho t})\mathrm{d}t\\&=Q_{KN}\left(\sqrt{2\rho},\sqrt{\frac{2\zeta}{\sigma^2}}\right),\end{aligned} \quad \text{(B.5)}$$

where $Q_n(y,z)$ is defined in (A.12).

## References


[1] K. S. Bialkowski, I. V. L. Clarkson, and S. D. Howard, "Generalized canonical correlation for passive multistatic radar detection," in *Proc. IEEE Statist. Signal Process. Workshop (SSP)*, Nice, France, Jun. 2011, pp. 417–420.

[2] N. Vankayalapati and S. Kay, "Asymptotically optimal detection of low probability of intercept signals using distributed sensors," *IEEE Trans. Aerosp. Electron. Syst.*, vol. 48, no. 1, pp. 737–748, Jan. 2012.

[3] H. D. Griffiths and C. J. Baker, "Passive coherent location radar systems. Part 1: Performance prediction," *Proc. Inst. Electr. Eng.--Radar Sonar Navig.*, vol. 152, no. 3, pp. 124–132, Jun. 2005.

[4] C. J. Baker, H. D. Griffiths, and I. Papoutsis, "Passive coherent location radar systems. Part 2: Waveform properties," *Proc. Inst. Electr. Eng.—Radar Sonar Navig.*, vol. 152, no. 3, pp. 160–168, Jun. 2005.

[5] M. Cherniakov, *Bistatic Radars: Emerging Technology*. New York, NY, USA: Wiley, 2008.

[6] A. Zaimbashi, M. Derakhtian, and A. Sheikhi, "GLRT-based CFAR detection in passive bistatic radar," *IEEE Trans. Aerosp. Electron. Syst.*, vol. 49, no. 1, pp. 134–159, Jan. 2013.

[7] J. Wang, H.-T. Wang, and Y. Zhao, "Direction finding in frequency-modulated-based passive bistatic radar with a four-element ad hoc antenna array," *IET Radar Sonar Navig.*, vol. 5, no. 8, pp. 807–813, Oct. 2011.

[8] Z. Zhao, X. Wan, Q. Shao, Z. Gong, and F. Cheng, "Multipath clutter rejection for digital radio mondiale-based HF passive bistatic radar with OFDM waveform," *IET Radar Sonar Navig.*, vol. 6, no. 9, pp. 867–872, Dec. 2012.

[9] P. E. Howland, "Target tracking using television-based bistatic radar," *Proc. Inst. Electr. Eng.—Radar Sonar Navig.*, vol. 146, no. 3, pp. 166–174, Jun. 1999.

[10] H.-T. Wang, J. Wang, and L. Zhang, "Mismatched filter for analogue TV-based passive bistatic radar," *IET Radar Sonar Navig.*, vol. 5, no. 5, pp. 573–581, Jun. 2011.

[11] H. Sun, D. K. P. Tan, Y. Lu, and M. Lesturgie, "Applications of passive surveillance radar system using cell phone base station illuminators," *IEEE Aerosp. Electron. Syst. Mag.*, vol. 25, no. 3, pp. 10–18, Mar. 2010.

[12] D. Poullin, "Passive detection using digital broadcasters (DAB, DVB) with COFDM modulation," *Proc. Inst. Electr. Eng.—Radar Sonar Navig.*, vol. 152, no. 3, pp. 143–152, Jun. 2005.

[13] H. A. Harms, L. M. Davis, and J. Palmer, "Understanding the signal structure in DVB-T signals for passive radar detection," in *Proc. IEEE Conf. Radar*, Arlington, VA, USA, May 2010, pp. 532–537.

[14] R. Tao, Z. Gao, and Y. Wang, "Side peaks interference supperssion in DVB-T based passive radar," *IEEE Trans. Aerosp. Electron. Syst.*, vol. 48, no. 4, pp. 3610–3619, Oct. 2012.

[15] J. E. Palmer, H. A. Harms, S. J. Searle, and L. M. Davis, "DVB-T passive radar signal processing," *IEEE Trans. Signal Process.*, vol. 61, no. 8, pp. 2116–2126, Apr. 2013.

[16] K. Polonen and V. Koivunen, "Detection of DVB-T2 control symbols in passive radar systems," in *Proc. IEEE 7th Sens. Array Multichannel Signal Process. Workshop (SAM)*, Hoboken, NJ, USA, Jun. 2012, pp. 309–312.

[17] P. E. Howland, D. Maksimiuk, and G. Reitsma, "FM radio based bistatic radar," *Proc. Inst. Electr. Eng.—Radar Sonar Navig.*, vol. 152, no. 3, pp. 107–115, Jun. 2005.

[18] K. S. Kulpa and Z. Czekala, "Masking effect and its removal in PCL radar," *Proc. Inst. Electr. Eng.—Radar, Sonar Navig.*, vol. 152, no. 3, pp. 174–178, June 2005.

[19] F. Colone, R. Cardinali, and P. Lombardo, "Cancellation of clutter and multipath in passive radar using a sequential approach," in *Proc. IEEE Conf. Radar*, Verona, NY, USA, Apr. 2006, pp. 393–399.

[20] R. Cardinali, F. Colone, C. Ferretti, and P. Lombardo, "Comparison of clutter and multipath cancellation techniques for passive radar," in *Proc. IEEE Radar Conf.*, Waltham, MA, USA, Apr. 2007, pp. 469–474.

[21] R. Tao, H. Z. Wu, and T. Shan, "Direct-path suppression by spatial filtering in digital television terrestrial broadcasting-based passive radar," *IET Radar Sonar Navig.*, vol. 4, no. 6, pp. 791–805, Dec. 2010.

[22] F. Colone, R. Cardinali, P. Lombardo, O. Crognale, A. Cosmi, A. Lauri, and T. Bucciarelli, "Space-time constant modulus algorithm for multipath removal on the reference signal exploited by passive bistatic radar," *IET Radar, Sonar Navig.*, vol. 3, no. 3, pp. 253–264, Jun. 2009.

[23] S. Gogineni, M. Rangaswamy, B. D. Rigling, and A. Nehorai, "Cramér-Rao bounds for UMTS-based passive multistatic radar," *IEEE Trans. Signal Process.*, vol. 1, no. 1, pp. 95–106, Jan. 2014.

[24] C. R. Berger, B. Demissie, J. Heckenbach, and P. Willett, "Signal processing for passive radar using OFDM waveforms," *IEEE J. Sel. Topics Signal Process.*, vol. 4, no. 1, pp. 226–238, Feb. 2010.

[25] G. C. Carter and A. H. Nuttall, "Statistics of the estimate of coherence," *Proc. IEEE*, vol. 60, no. 4, pp. 465–466, Apr. 1972.

[26] G. C. Carter, "Estimation of the magnitude-squared coherence function (Spectrum)," Naval Underwater Systems Center, New London Lab., New London, CT, USA, Tech. Rep. 4343, May 1972.
[27] G. C. Carter, C. H. Knapp, and A. H. Nuttall, "Estimation of the magnitude-squared coherence function via overlapped fast Fourier transform processing," *IEEE Trans. Audio Electroacoust.*, vol. AU-21, no. 4, pp. 337–344, Aug. 1973.
[28] G. C. Carter, "Coherence and time delay estimation," *Proc. IEEE*, vol. 75, no. 2, pp. 236–255, Feb. 1987.
[29] R. D. Trueblood and D. L. Alspach, "Multiple coherence as a detection statistic," Naval Ocean Syst. Center, Tech. Rep. NOSC 265, 1978.
[30] H. Gish and D. Cochran, "Invariance of the magnitude-squared coherence estimate with respect to second-channel statistics," *IEEE Trans. Acoust., Speech, Signal Process.*, vol. ASSP-35, no. 12, pp. 1774–1776, Dec. 1987.
[31] S. Wang and M. Tang, "Exact confidence interval for magnitude-squared coherence estimates," *IEEE Signal Process. Lett.*, vol. 11, no. 3, pp. 326–329, Mar. 2004.
[32] H. Gish and D. Cochran, "Generalized coherence," in *Proc. Int. Conf. Acoust., Speech, Signal Process.*, New York, NY, USA, Apr. 1988, pp. 2745–2748.
[33] D. Cochran and H. Gish, "Multiple-channel detection using generalized coherence," in *Proc. Int. Conf. Acoust., Speech, Signal Process.*, Albuquerque, NM, USA, Apr. 1990, pp. 2883–2886.
[34] D. Cochran, H. Gish, and D. Sinno, "A geometric approach to multichannel signal detection," *IEEE Trans. Signal Process.*, vol. 43, no. 9, pp. 2049–2057, Sep. 1995.
[35] A. Clausen and D. Cochran, "Asymptotic analysis of the generalized coherence estimate," *IEEE Trans. Signal Process.*, vol. 49, no. 1, pp. 45–53, Jan. 2001.
[36] S. Sirianunpiboon, S. D. Howard, and D. Cochran, "A Bayesian derivation of generalized coherence detectors," in *Proc. Int. Conf. Acoust., Speech, Signal Process.*, Kyoto, Japan, Mar. 2012, pp. 3253–3256.
[37] K. S. Bialkowski and I. V. L. Clarkson, "Passive radar signal processing in single frequency networks," in *Proc. 46th Asilomar Conf. Signals, Syst. Comput.*, CA, Nov. 2012, pp. 199–202.
[38] M. A. Richards, J. A. Scheer, and W. A. Holm, *Principles of Modern Radar: Basic Principles*. New York, NY, USA: Scitech, 2010.
[39] E. J. Kelly, "An adaptive detection algorithm," *IEEE Trans. Aerosp. Electron. Syst.*, vol. 22, no. 1, pp. 115–127, Mar. 1986.
[40] A. Kortun, M. Sellathurai, T. Ratnarajah, and C. Zhong, "Distribution of the ratio of the largest eigenvalue to the trace of complex Wishart matrices," *IEEE Trans. Signal Process.*, vol. 60, no. 10, pp. 5527–5532, Oct. 2012.
[41] P. A. Dighe, R. K. Mallik, and S. S. Jamuar, "Analysis of transmit-receive diversity in Rayleigh fading," *IEEE Trans. Commun.*, vol. 51, no. 4, pp. 694–703, Apr. 2003.
[42] A. Maaref and S. Aissa, "Closed-form expression for the outage and ergodic Shannon capacity of MIMO MRC systems," *IEEE Trans. Commun.*, vol. 53, no. 7, pp. 1092–1095, Jul. 2005.
[43] C. G. Khatri, "Distribution of the largest or the smallest characteristic root under null hypothesis concerning complex multivariate normal populations," *Ann. Math. Statist.*, vol. 35, no. 4, pp. 1807–1810, Dec. 1964.
[44] M. Kang and M.-S. Alouini, "Largest eigenvalue of complex Wishart matrices and performance analysis of MIMO MRC systems," *IEEE J. Sel. Areas Commun.*, vol. 21, no. 3, pp. 418–426, Apr. 2003.
[45] A. H. Nuttall, "Some integrals involving the $Q$ function," Naval Underwater Systems Center, New London Lab., New London, CT, USA, Tech. Rep. 4297, 1972.
[46] M. K. Simon, "The Nuttall $Q$ function—Its relation to the Marcum $Q$ function and its application in digital communication performance evaluation," *IEEE Trans. Commun.*, vol. 50, no. 11, pp. 1712–1715, Nov. 2002.
[47] A. H. Nuttall, "Some integrals involving the $Q_M$ function," Naval Underwater Systems Center, New London Lab., New London, CT, USA, Tech. Rep. AD-779 846, May 1974.

**Jun Liu** (S'11–M'13) received the B.S. degree in mathematics from Wuhan University of Technology, China, in 2006, the M.S. degree in mathematics from Chinese Academy of Sciences, in 2009, and the Ph.D. degree in electrical engineering from Xidian University, China, in 2012.

From July 2012 to December 2012, he was a Postdoctoral Research Associate in the Department of Electrical and Computer Engineering, Duke University, Durham, NC. From January 2013 to September 2014, he was a Postdoctoral Research Associate in the Department of Electrical and Computer Engineering, Stevens Institute of Technology, Hoboken, NJ. He is now with the National Laboratory of Radar Signal Processing, Xidian University, where he is an Associate Professor. His current research interests include statistical signal processing, optimization algorithms, passive sensing, cognitive radar, and multistatic radar.

**Hongbin Li** (M'99–SM'08) received the B.S. and M.S. degrees from the University of Electronic Science and Technology of China, in 1991 and 1994, respectively, and the Ph.D. degree from the University of Florida, Gainesville, in 1999, all in electrical engineering.

From July 1996 to May 1999, he was a Research Assistant in the Department of Electrical and Computer Engineering at the University of Florida. Since July 1999, he has been with the Department of Electrical and Computer Engineering, Stevens Institute of Technology, Hoboken, NJ, where he is a Professor. He was a Summer Visiting Faculty Member at the Air Force Research Laboratory in the summers of 2003, 2004, and 2009. His general research interests include statistical signal processing, wireless communications, and radars.

Dr. Li received the IEEE Jack Neubauer Memorial Award in 2013 for the best systems paper published in the IEEE TRANSACTIONS ON VEHICULAR TECHNOLOGY, the Outstanding Paper Award from the IEEE AFICON Conference in 2011, the Harvey N. Davis Teaching Award in 2003 and the Jess H. Davis Memorial Award for Excellence in Research in 2001 from Stevens Institute of Technology, and the Sigma Xi Graduate Research Award from the University of Florida in 1999. He has been a member of the IEEE SPS Signal Processing Theory and Methods (2011 to now) Technical Committee (TC) and the IEEE SPS Sensor Array and Multichannel TC (2006–2012). He is an Associate Editor for *Signal Processing* (Elsevier), and served on the editorial boards for IEEE TRANSACTIONS ON WIRELESS COMMUNICATIONS, IEEE SIGNAL PROCESSING LETTERS, and IEEE TRANSACTIONS ON SIGNAL PROCESSING. He was a Guest Editor for EURASIP *Journal on Applied Signal Processing*. He has been involved in various conference organization activities, including serving as a General Co-Chair for the 7th IEEE Sensor Array and Multichannel Signal Processing (SAM) Workshop, Hoboken, NJ, June 17–20, 2012. He is a member of Tau Beta Pi and Phi Kappa Phi.

**Braham Himed** (S'88–M'90–SM'01–F'07) received the B.S. degree in electrical engineering from Ecole Nationale Polytechnique of Algiers in 1984, and the M.S. and Ph.D. degrees both in electrical engineering, from Syracuse University, Syracuse, NY, in 1987 and 1990, respectively.

He is a Technical Advisor with the Air Force Research Laboratory, Sensors Directorate, RF Technology Branch, in Dayton OH, where he is involved with several aspects of radar developments. His research interests include detection, estimation, multichannel adaptive signal processing, time series analyses, array processing, space-time adaptive processing, waveform diversity, MIMO radar, passive radar, and over the horizon radar.

Dr. Himed is the recipient of the 2001 IEEE Region I award for his work on bistatic radar systems, algorithm development, and phenomenology. He is a member of the AES Radar Systems Panel and a Fellow of AFRL (Class of 2013). He is a recipient of the 2012 IEEE Warren White award for excellence in radar engineering.